Journal of Renewable Materials

Tech Science Press

DOI: 10.32604/jrm.2024.055437

ARTICLE

Revolutionizing Biodegradable and Sustainable Materials: Exploring the Synergy of Polylactic Acid Blends with Sea Shells

Prashanth K P[1,*], Rudresh M[2], Venkatesh N[3], Poornima Gubbi Shivarathri[4] and Shwetha Rajappa[5]

[1]Department of Mechanical Engineering, Acharya Institute of Technology, Bangalore, 560107, India

[2]Department of Robotics and Artificial Intelligence, Dayananda Sagar College of Engineering, Bangalore, 560111, India

[3]Department of Mechanical Engineering, University of Visvesvaraya College of Engineering, Bangalore, 560001, India

[4]Department of Chemistry, New Horizon College of Engineering, Bangalore, 560103, India

[5]Department of Sciences and Humanities, Christ (Deemed to be University), Bangalore, 560074, India

[*]Corresponding Author: Prashanth K P. Email: prashanthkp@acharya.ac.in

Received: 27 June 2024 Accepted: 14 October 2024 Published: 20 December 2024

ABSTRACT

This study explores the mechanical properties of a novel composite material, blending polylactic acid (PLA) with sea shells, through a comprehensive tensile test analysis. The tensile test results offer valuable insights into the material's behavior under axial loading, shedding light on its strength, stiffness, and deformation characteristics. The results suggest that the incorporation of sea shells decrease the tensile strength of 14.55% and increase the modulus of 27.44% for 15 wt% SSP (sea shell powder) into PLA, emphasizing the reinforcing potential of the mineral-rich sea shell particles. However, a potential trade-off between decreased strength and reduced ductility is noted, highlighting the need for a delicate balance in material composition. The study underscores the importance of uniform sea shell particle distribution within the PLA matrix for consistent mechanical performance. These results offer a basis for additional PLA-sea shell blend optimization, directing future efforts to balance strength, flexibility, and other critical attributes for a range of applications, including biomedical devices and sustainable packaging. This investigation opens the door to more sustainable and mechanically strong materials in the field of additive manufacturing by demonstrating the positive synergy between nature-inspired materials and cutting-edge testing techniques.

KEYWORDS

PLA; sea shell; additive manufacturing; tensile; flexural; biodegradability

1 Introduction

A thermoplastic that breaks down biodegradable using renewable resources like sugarcane or corn starch is called poly (lactic acid) (PLA). PLA is now a top contender in the biopolymer industry thanks to its advantageous mechanical qualities and environmental friendliness, particularly when it comes to lowering reliance on plastics made from fossil fuels. PLA-based composites have drawn a lot of interest because of its potential for use in a variety of products, including automotive components and packaging. Notwithstanding these benefits, the PLA composites that are now available on the market have several significant drawbacks.

Engineers and scientists are always looking into novel materials and blends that not only decrease environmental effect but also harness the power of nature's resources in their quest for sustainable alternatives to standard plastics. Combining sea shells with polylactic acid (PLA), a renewable and biodegradable polymer, is one such intriguing line of inquiry. It may seem strange, but the combination works surprisingly well. This study delves into the innovative application of PLA composites blended with seashells, highlighting their unique mechanical properties and significant environmental advantages, and possible uses that make this combination a ray of hope in the ongoing fight against plastic pollution [1–4].

Because of its intrinsic brittleness and comparatively low thermal stability, PLA presents a number of difficulties and restricts its use in high-performance settings. Additionally, despite being a major benefit, PLA's biodegradability has a drawback in terms of mechanical durability when compared to non-biodegradable polymers. In order to improve the mechanical, thermal, and barrier qualities of PLA, the market for PLA composites has been investigating a variety of fillers and reinforcements, including natural fibers, nanoclays, and other biobased materials. However, these initiatives frequently come with trade-offs that prevent widespread adoption, such reduced biodegradability or higher production costs [5–8].

Using elements from the marine environment, especially seashells shown in Fig. 1, as a filler in PLA composites is a potential but little-studied approach. The main material that makes up seashells is calcium carbonate ($CaCO_3$), which is renowned for its stiffness and heat resilience. Seashell powder can be added to PLA to improve the composite's mechanical qualities, such as impact resistance and tensile strength, without seriously affecting its biodegradability. Seashells are also a plentiful and underutilized waste resource, especially in coastal areas, which makes them an affordable and sustainable choice for reinforcement.

Figure 1: Sea shell powder

Because seashells are an easily accessible and frequently discarded resource, they present a chance for recycling and waste reduction, helping to address the problem of marine litter. Because seashells are high in calcium carbonate, they increase the mechanical strength of material blends and improve the resilience and

durability of PLA-seashell composites in demanding applications. By reusing natural materials and lowering the demand for new resources, the incorporation of seashells adheres to environmental sustainability principles. Additionally, by reusing marine debris in manufacturing processes, it contributes to the preservation of ocean habitats.

Seashells and PLA work together to improve the material blend's mechanical strength and endurance, solving PLA's common drawbacks and increasing its potential applications. By combining a biodegradable polymer with an ocean-sourced waste material, this combination also preserves an environmentally favorable image, promoting a circular economy and reducing environmental impact. The PLA-seashell blend, which offers a compelling substitute for traditional plastics and advances the development of a more sustainable future, is an example of how innovative material solutions can align with environmental responsibility. Its promising applications range from biodegradable medical implants to sustainable packaging [9].

The mechanical properties of polylactic acid (PLA) blends are important in the development of sustainable materials because they influence how well-suited the blends are for different applications. It is crucial to assess the mechanical performance of the combined PLA and sea shell powder (SSP) material, especially with regard to its tensile and flexural qualities. The material's strength and elongation under uniaxial strain are measured during tensile testing, which gives information about the material's capacity to bear stretching forces without breaking. Conversely, flexural testing evaluates the material's response under bending stress, exposing its stiffness and ability to withstand deformation. Researchers can ascertain the impact of sea shell powder incorporation on the mechanical integrity of PLA-SSP blends by performing tensile and flexural tests on the material. These evaluations are essential to guaranteeing that PLA-SSP composites contribute to environmental sustainability while also fulfilling the performance requirements for the packaging and agricultural film applications for which they are designed [10,11].

The biodegradability of different blends of polylactic acid (PLA) and seashell powder (SSP) can be evaluated by the utilization of hydrolytic and oxidative reagents, providing significant insights into their environmental impact. Hydrolytic reagents release lactic acid and mimic the hydrolysis of ester bonds in PLA, giving an indication of the material's degradation in damp settings. For applications where biodegradability is critical, testing these blends under such circumstances is essential. The addition of SSP in varying ratios may affect this process. However, by adding reactive oxygen species, oxidative reagents-such as Fenton's reagent-imitate oxidative breakdown. This is especially important for figuring out how PLA-SSP blends function in conditions where oxidative stress is common. These tests are crucial for ascertaining the PLA-SSP blends' overall environmental sustainability and guaranteeing that they fulfill environmental objectives and particular biodegradability standards, particularly in applications exposed to outdoor settings like agricultural films or disposable goods. The results of these investigations serve as a basis for the creation of PLA-based materials that support environmental sustainability while also meeting regulatory requirements [12].

The research's theory is that adding seashell powder to PLA may boost the material's mechanical and thermal characteristics while preserving its biodegradability, making it better suited for uses needing increased durability. With its innovative method, PLA composites may be able to overcome their present market shortcomings and provide a more environmentally friendly and functionally sound material substitute.

2 Materials and Method

In materials science, polylactic acid (PLA) and seashells make an eco-friendly and fascinating combination. Each ingredient contributes special qualities to the blends, creating a material that not only overcomes the drawbacks of conventional plastics but also makes use of the advantages of natural, renewable resources. Tables 1 and 2 represents the properties of PLA [13] and sea shell [14–18], respectively.

Table 1: Properties of PLA

Property	Values
Viscosity	0.256–0.467 MPs-s
Density	1.25 g/cm^3 at 21.5°C
Thermal conductivity	0.13 W/M-K
Thermal diffusivity	0.056 m^2/s
Specific heat	180 L/kg-K
Feed rate	2.247–2.67 m/s
Yield tensile strength	52 MPa
% Elongation at yield	10%–100%
Flexural modulus	345–450 MPa
Melting point	120°C–170°C
Glass transition temperature	54°C–56°C
Shear modulus	2.4 GPa

Table 2: Properties of sea-shell powder per 100 gm

Property	Values
Silicon dioxide	1.60
Alumina	0.92
Calcium carbonate	51.56
Magnesium oxide	1.43
Sodium oxide	0.08
Potassium oxide	0.06
Water	0.31
LOI	41.84

In the field of additive manufacturing, the combination of polylactic acid (PLA) and seashells via filament extrusion and subsequent 3D printing is innovative [19]. It's crucial to remember that the precise outcomes would depend on a number of variables, including the proportion of PLA to seashells, the size and distribution of the seashell particles, and the processing settings used to make the material. These findings must be validated by real testing in a lab environment and should be regarded as hypothetical [20–24].

2.1 Filament Extrusion Process

2.1.1 Material Preparation

A composite feedstock is made by combining seashell particles that have been finely ground to a size range between 10 to 100 micrometers (μm) with PLA pellets that come from sustainable sources.

2.1.2 Extrusion Blending

The feedstock for the composite is supplied into an extruder, where it is melted and blended under controlled conditions such as temperature, pressure, shear rate, feed rate, residence time and cooling rate. To guarantee that the sea shell particles are distributed uniformly throughout the PLA matrix, precise pressure and temperature parameters are maintained. The temperature in the Feed Zone (Zone 1) is usually kept between 170°C–180°C so that the PLA can soften and start combining with the seashell particles. The temperature is raised to 180°C–190°C as the material enters the Compression Zone (Zone 2), further melting the PLA and accelerating the mixing process to encourage uniform particle distribution. In the Metering Zone (Zone 3), shear forces are optimized to guarantee a uniform dispersion of seashell particles throughout the PLA matrix, and the temperature is kept between 190°C and 200°C, at which point the material melts completely. Finally, the Nozzle Temperature is set at 200°C–210°C, ensuring the composite material is properly melted and smoothly extruded into a filament [25–28]. The extruder's extrusion pressure is normally kept between 50 and 150 bar, which is sufficient force to prevent backpressure, which could cause blockages or uneven material flow, while the molten PLA and seashell combination are still flowing through the extruder. The pressure is usually regulated between 20 and 50 bar at the die, where the filament is formed. In order to ensure that the seashell particles are evenly dispersed and that the filament has a smooth, superior surface finish, this reduced pressure aids in the consistent extrusion process. Furthermore, the screw speed which is typically regulated between 50 and 100 rpm can also be changed to modify the shear rate. The dispersion of seashell particles within the PLA matrix is further enhanced by larger shear stresses, which are caused by a higher screw speed [29–31].

2.1.3 Filament Formation

After that, a die is used to extrude the melted mixture into filaments under controlled cooling conditions with the required diameter typically around 0.15 or 0.4 mm. The filaments produce a PLA-sea shell composite filament that is ready for 3D printing after cooling and solidifying [32–36].

Table 3 represents the process parameter used for 3D printing, and Table 4 represents the test sample material % details generated for the structural and mechanical characterization [37,38].

Table 3: The parameters of the 3D printing process

Compaction density of the sample	100%
Nozzle diameter	0.4 mm
Fill pattern	Line
Fill angle	45°
Layer thickness	0.15 mm
Speed	60 m/sec

Table 4: Details of the material % in test samples

Sample number	Material % details	Sample code
Sample 1	PLA	PLA
Sample 2	90% PLA + 10% seashell powder	PLASS10
Sample 3	85% PLA + 15% seashell powder	PLASS15
Sample 4	80% PLA + 20% seashell powder	PLASS20

3 Experimentation

3.1 Tensile

Conducting tensile test on a material in this example, a composite of seashells and polylactic acid (PLA) offers important insights on the material's mechanical characteristics and behavior under tension. Tensile tests examine a sample's response to stress and strain by subjecting it to axial loading, usually by ripping it apart.

The BISS Nano Plug-n-Play line of test systems for servohydraulics underwent a tensile test. Regarding the tensile test, the most popular specimen, ASTM D638-at a constant traverse rate of 1 mm/min, a constant rectangular cross-section with measurements of 19 mm in width, 115 mm in length, and 4 mm in depth is employed in the moving grip. To stop gripping damage, additional tabs can be glued to the specimen's ends [39,40]. Fig. 2 represents the tensile test specimens (a) PLA and (b) PLA + SSP (10%, 15%, and 20%).

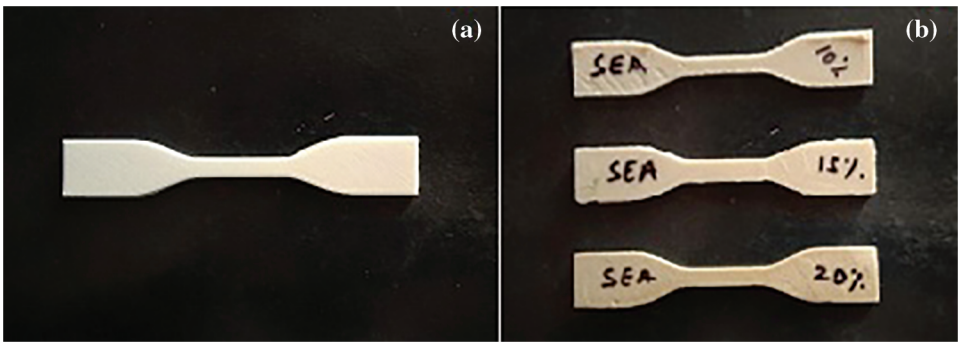

Figure 2: Tensile test specimen (a) PLA (b) 90%PLA + 10%SSP, 85%PLA + 15%SSP, 80%PLA + 20%SSP

3.2 Flexural

The standard specimen thickness for the flexural test is 4 mm (0.16 in), the standard specimen width is 10 mm (0.39 in), and the standard specimen length is 80 mm. ASTM D790 was taken into consideration. In the event that the standard specimen is unavailable, ISO 178 provides substitute widths based on the thickness of the specimen [41]. The flexural test specimen is displayed in Fig. 3. (a) PLA (b) PLA with 10%, 15%, and 20% SSP added.

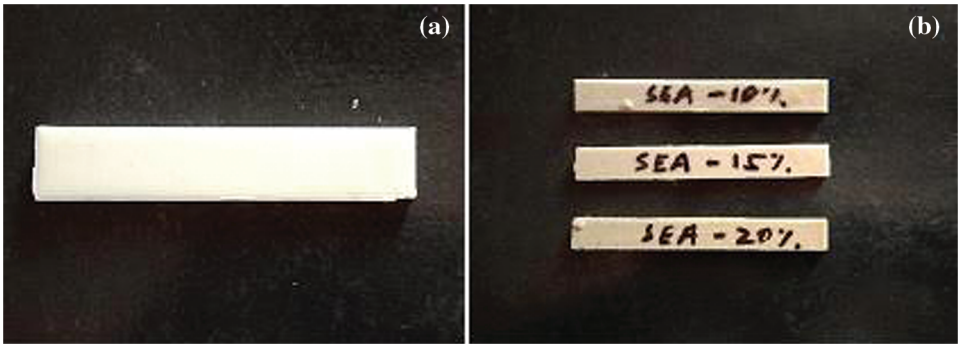

Figure 3: Flexural test samples (a) PLA (b) 90%PLA + 10%SSP, 85%PLA + 15%SSP, 80%PLA + 20%SSP

3.3 Biodegradability

To determine if the composite was biodegradable, a test for biodegradability was performed on the samples [42,43]. Using the ISO 10993 standard, biodegradability is determined. Three tests are recommended by the standard to ascertain the biodegradability rate.

- Test for Hydrolytic Degradation: This test determines whether a composite is degradable using water.
- Test for Oxidative Degradation: This test uses a 3% Pharmacopoeia-grade hydrogen peroxide mixture in addition to water.
- Test for Fenton's Reagent: This involves mixing iron salts with a diluted solution of hydrogen peroxide.

Buffer solution deterioration tests include Fenton's Reagent test and Oxidative deterioration test.

A ratio of 10:1 should be used to compare the test specimen's mass and the test solution's volume. A pH meter was used, and a pH range was selected in order to maintain the properties of the medium. The test item is dried and its mass is noted before any experiments are conducted. The specimen is dried and then cleaned with analytical grade water after it has been in solution for the necessary amount of time. After that, the mass is weighed before being further considered.

3.4 Scanning Electron Microscope and X-Ray Diffraction

The morphologic of the PLA/SSP illustrations of composite from the outer layers enlarged 1000× was examined using a SEM. Utilizing a JSM 6700F SEM, captured the fractography of the thin, gold-sputtered, brittle composite films [44–46]. Wide-angle XRD of PLA and PLA/SSP composite films were taken. The device consists of a rotating anode generator equipped with a broad-angle goniometer and a copper target. The generator scanned the samples in the 2theta range of 10° to 90° while driving at 30 mA and 40 kV. The sample-to-detector distance, or 141 mm Goniometer Radius, influences the accuracy of angle measurements. The analysis was performed over a Runtime of 2244.409 s with a step size of 0.025 degrees, a theta angle of 4.998997 degrees, and a corresponding 2theta value of 9.997994 degrees. Throughout the analysis, the rotation speed was maintained at five revolutions per minute [47–49].

4 Results and Conversations

The PLA-based composite films were flexible, showed no obvious cracks, and were well-processable during 3D printing. The PLA composite films reinforced with SSP were evenly applied to the surfaces, preserving the appearance of the sheets, and the thickness remained unaffected by the SSP's presence.

4.1 Tensile

Tensile strength is the maximum weight per unit area pushed in a given direction along a specimen's length that it can withstand without breaking. To ascertain the mechanical performance of PLA/SSP composite films, the tensile characteristics were examined. Figs. 4–7 display the PLA and PLA/SSP composite films' tensile test curves. Table 3 shows the effect of filler loading on the tensile properties (elongation at break, modulus, and strength) of PLA composite films filled with SSP. Tension strength diminished with filler levels up to 20%, whereas modulus increased with the amount of filler up to 15% before subsequently dropping. As filler quantity is increased, strength and modulus drop due to filler agglomeration and a weaker filler-matrix interaction, which could be the cause of this discontinuity. This is probably attributable to the effect of van der Waals or induction relationships, which enhance the bond that exists between the filler and the matrix. Conversely, the tension strength and modulus of the composite film were identified to be consistently elevated than those of the matrix.

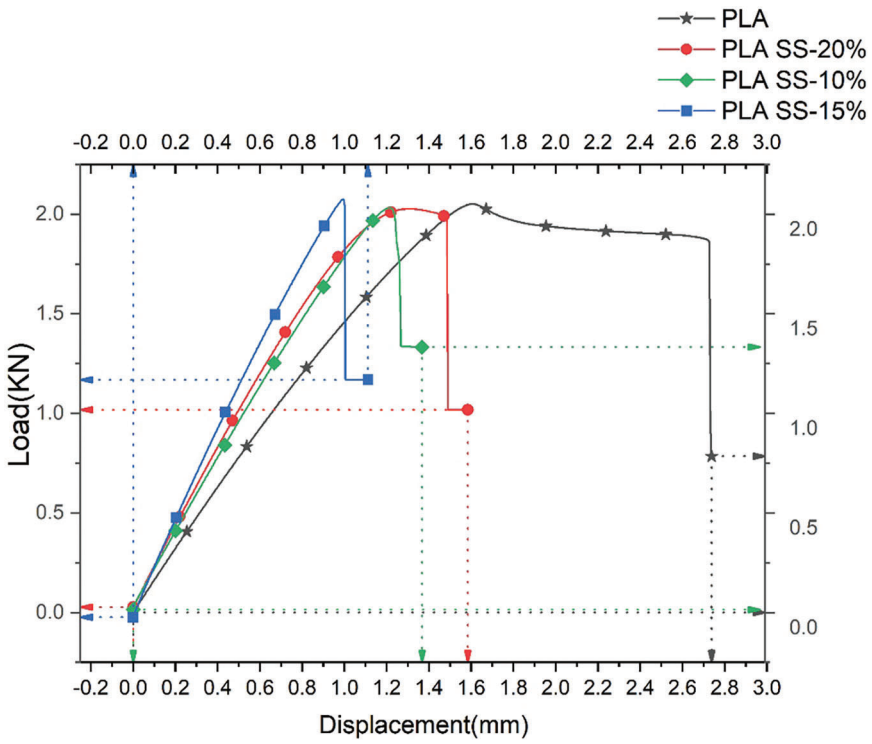

Figure 4: Tensile test-load *vs*. displacement visual depiction of PLA and its blends

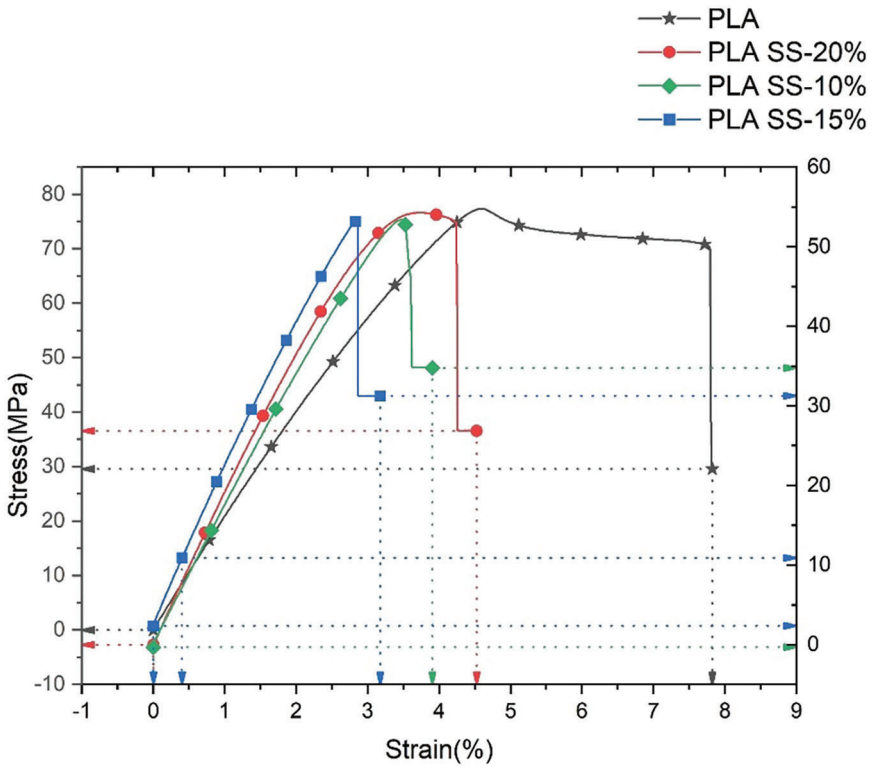

Figure 5: Tensile test-stress *vs*. strain visual depiction of PLA and its blends

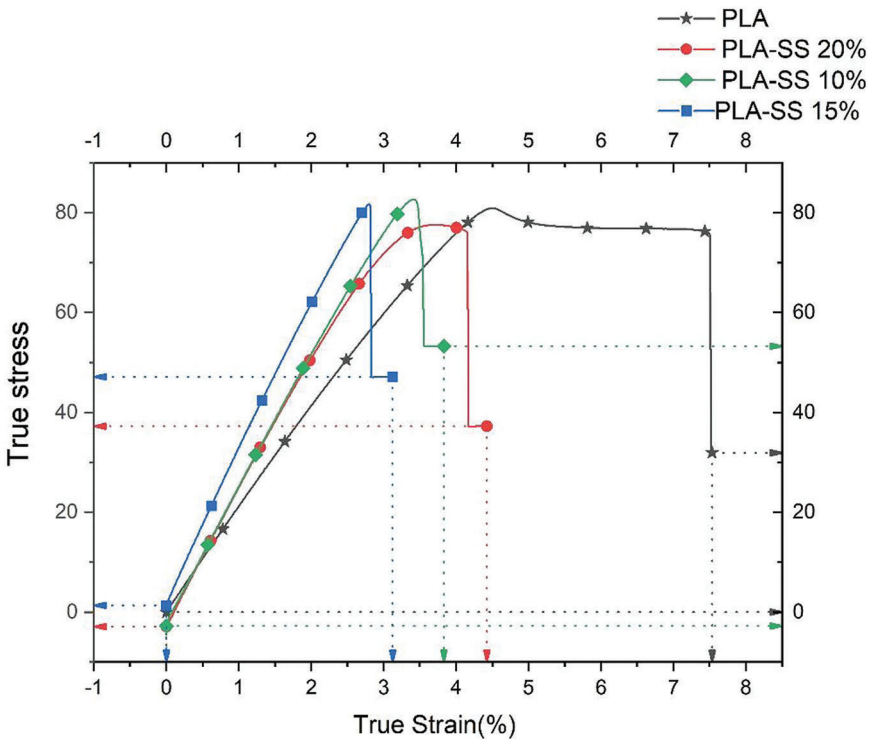

Figure 6: Tensile test-true stress *vs*. true strain visual depiction of PLA and its blends

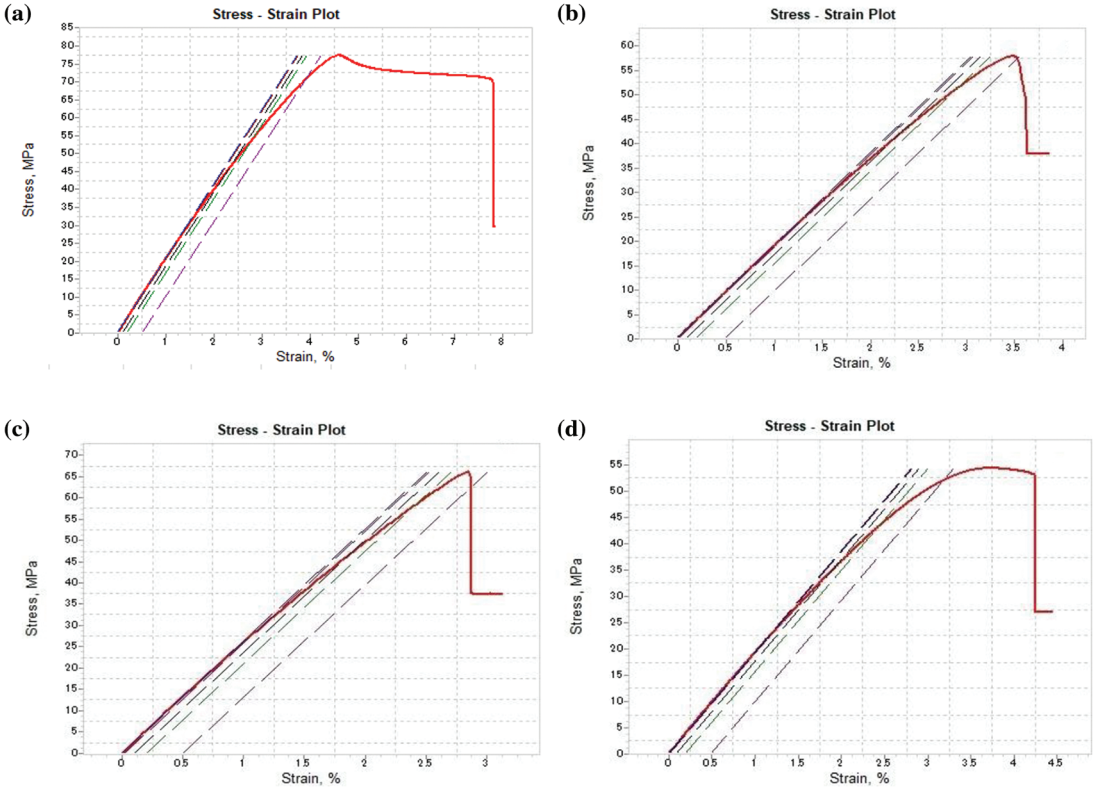

Figure 7: Visual depiction of offset yield stress-strain plot (a) PLA, (b) PLA (90%) + SSP (10%), (c) PLA (85%) + SSP (15%), (d) PLA (80%) + SSP (20%)

As the percentage of Sea Shell Powder (SSP) in the PLA matrix rises, the Peak Stress continuously falls. The reduction in stress from 77.379 to 54.291 MPa is noteworthy when switching from pure PLA to PLA (80%) with SSP (20%) as shown in Table 5. This suggests that adding SSP causes the material's peak strength to decrease; PLA (80%) + SSP (20%) shows the lowest value. The 0.2% Offset Yield Stress gradually decreases with increasing SSP content, much like Peak Stress does. In comparison to the pure PLA result of 54.413 MPa, PLA (80%) + SSP (20%) shows the lowest yield stress at 47.407 MPa, indicating a continuing trend of decreased resistance to plastic deformation.

Table 5: Tensile test results for different composition of sea shell in a PLA matrix

Parameters	PLA	PLA (90%) + SSP (10%)	PLA (85%) + SSP (15%)	PLA (80%) + SSP (20%)
Peak stress (MPa)	77.379	57.874	66.116	54.291
Peak load (KN)	2.052	1.535	1.753	1.44
0.2% Offset yield stress (MPa)	54.413	51.562	58.636	47.407
0.5% Offset yield stress (MPa)	70.828	57.236	37.494	52.181
Modulus (GPa)	2.066	1.885	2.633	1.924
Upper yield point (MPa)	54.413	51.562	58.636	43.407
Lower yield point (MPa)	76.774	37.855	37.42	54.242
Strain hardening coefficient (MPa)	278.89	147.033	306.228	118.219
Elongation at break (Using strain) (%)	7.822	3.843	3.109	4.446
Stiffness (kN/mm)	1.565	1.428	1.995	1.458

As the SSP concentration rises, the modulus, which measures the material's stiffness, tends to decrease. The modulus of PLA (85%) + SSP (15%) is 2.633 GPa, the greatest, while PLA (80%) + SSP (20%) is the lowest, at 1.924 GPa. As expected that the stiffness of the material is impacted by the addition of SSP. As SSP concentration rises, the Upper Yield Point, a crucial marker of the beginning of plastic deformation, falls. The lowest result, 43.407 MPa, is shown by PLA (80%) + SSP (20%), highlighting the material's decreasing capacity to withstand plastic deformation. With increased SSP content, there is a noticeable decrease in the material's capacity for plastic deformation, as indicated by the Strain Hardening Coefficient. In terms of strain hardening capability, PLA (85%) + SSP (15%) has the maximum value at 306.228 MPa, while PLA (80%) + SSP (20%) has the lowest value at 118.219 MPa. As the SSP concentration rises, stiffness—a measure of resistance to deformation—consistently falls. At 1.995 kN/mm, PLA (85%) + SSP (15%) exhibits the maximum stiffness, whereas PLA (80%) + SSP (20%) exhibits the lowest stiffness, at 1.458 kN/mm. This suggests that when the proportion of SSP increases, the material becomes less stiff. When SSP is added by 10, 15 and 20 wt% into PLA, we observed tensile strength is decreased by 25.20%, 14.55% and 29.83% respectively compared with the PLA. It can be observed that the young's modulus of 15 wt% SSP blend with PLA is increased by 27.44% compared with the PLA. Therefore for composite, tensile strength enhancement is directly proportional to amount of SSP and the effect of SSP has only influence on tensile modulus.

4.2 Flexural

Figs. 8–10 displays the PLA and PLA/SSP composite films' flexural test curves. All of the compositions show a different pattern for the Flexural Peak Stress. Interestingly, the addition of SSP to PLA (90%) + SSP (10%) and PLA (85%) + SSP (15%) results in a significant drop to 13.765 and 10.258 MPa, respectively, whereas PLA has a Flexural Peak Stress of 48.542 MPa. The Flexural Peak Stress in PLA (80%) + SSP (20%) increases to 49.486 MPa, which is an interesting increase. This suggests that there is a complicated link between flexural strength and the PLA-SSP ratio. A similar pattern can be seen in the Offset Flexural Yield Stress, which shows a notable drop from 39.224 MPa in pure PLA to 13.169 and 9.936 MPa in PLA (90%) + SSP (10%) and PLA (85%) + SSP (15%), respectively. After that, PLA (80%) + SSP (20%) exhibits a marginal increase to 39.933 MPa. This implies that the material's capacity to withstand yielding under flexural stress may be significantly impacted by the addition of SSP. The material's stiffness can be inferred from the Tangent Modulus, which is the stress-strain curve's slope. Here, the addition of SSP results in a significant drop. PLA has the largest Tangent Modulus at 1.895 GPa, but the lowest at 0.105 GPa are shown by PLA (85%) + SSP (15%) and PLA (90%) + SSP (10%). A slightly greater Tangent Modulus at 0.165 GPa is shown by PLA (80%) + SSP (20%), suggesting a complex link between PLA-SSP ratios and the material's stiffness under flexural loading. To sum up, these results emphasize how PLA and SSP interact intricately to influence flexural properties, highlighting the importance of carefully considering material composition to achieve desired mechanical characteristics. Table 6 shows the Flexural test results for different composition of sea shell in a PLA matrix.

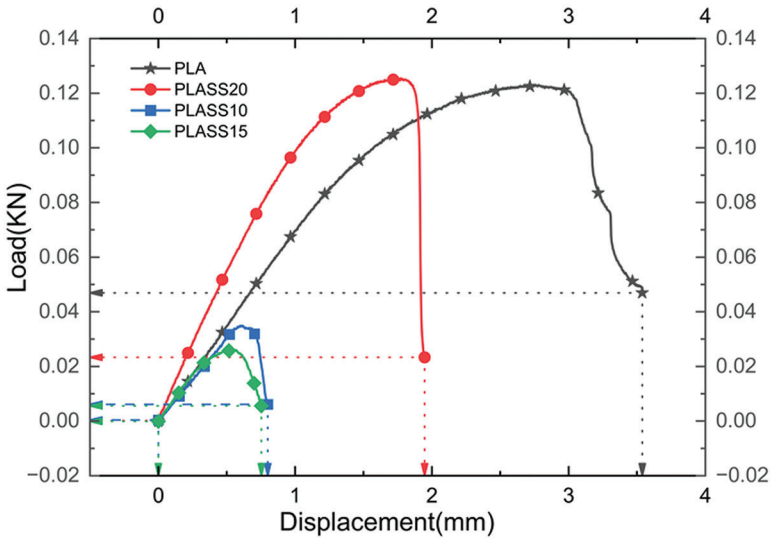

Figure 8: Flexural test graphs-load *vs*. displacement for PLA and its blends

4.3 Biodegradability

Strong bases like KOH or NaOH can usually be used as reagents in hydrolytic processes. The PLA's active groups became water-sensitive when the base OH reacted with both PLA and reinforced PLA, particularly with polylactic acid that had absorbed a considerable amount of moisture. Depending on the chemical structure, it perceives the water in a different way. From that point on, as seen in Fig. 11a, it starts to get worse every day. As the number of days grows, the bulk of the materials reduces.

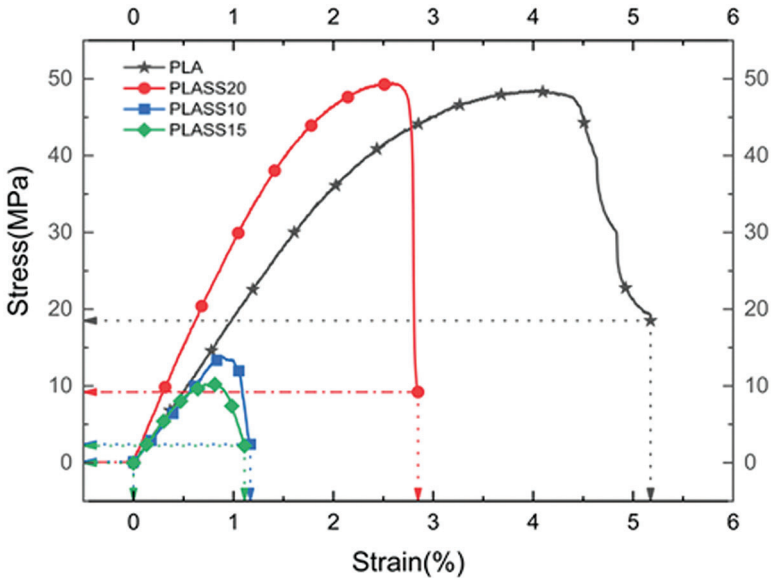

Figure 9: Flexural test graphs-stress *vs*. strain for PLA and its blends

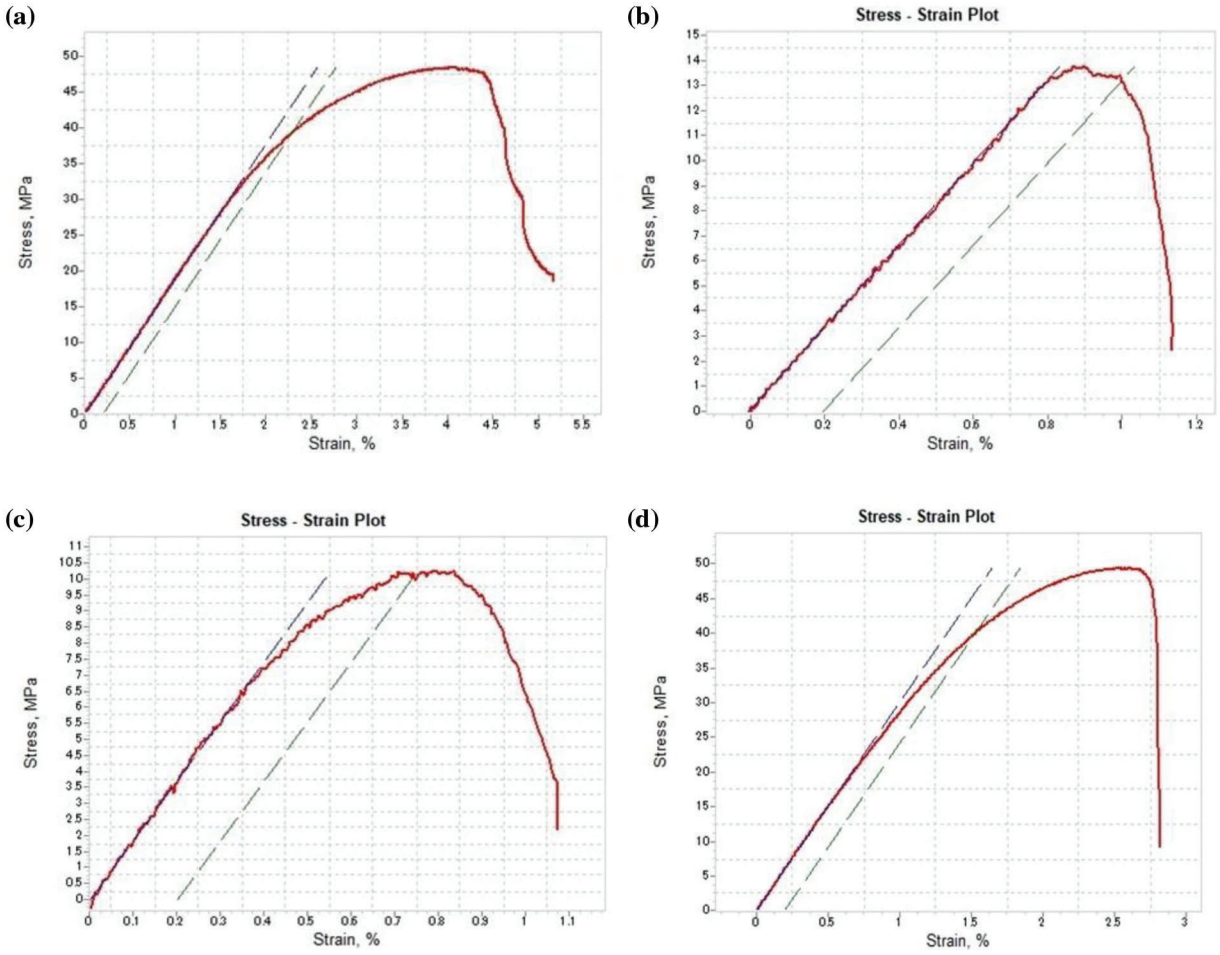

Figure 10: Flexural test graphs-offset yield stress-strain plot for (a) PLA, (b) PLA (90%) + SSP (10%), (c) PLA (85%) + SSP (15%), (d) PLA (80%) + SSP (20%)

Table 6: Flexural test results for different composition of sea shell in a PLA matrix

Parameters	PLA	PLA (90%) + SSP (10%)	PLA (85%) + SSP (15%)	PLA (80%) + SSP (20%)
Flexural peak stress (MPa)	48.542	13.765	10.258	49.486
Flexural yield stress offset (MPa)	39.224	13.169	9.936	39.933
Tangent modulus (GPa)	1.895	0.105	0.105	0.165
At break flexural stress (MPa)	18.504	2.415	2.192	9.2

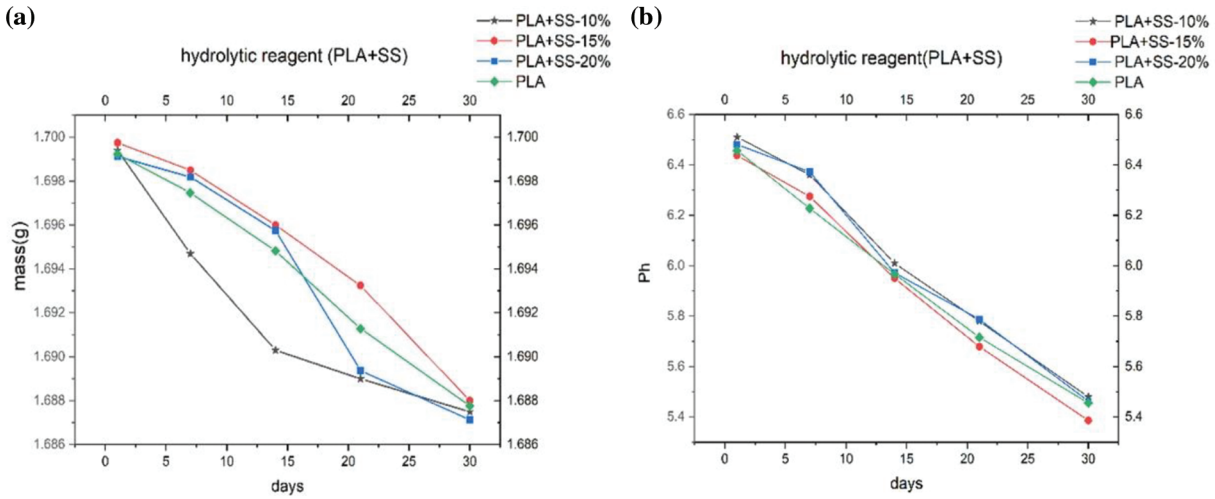

Figure 11: Biodegradability test using hydrolytic reagent (a) Mass *vs*. days (b) pH *vs*. days

The strong base in the solution causes the materials' pH to fall with increasing days, as shown in Fig. 11b. Since acidity and concentration have an inverse relationship with pH, the powerful base diminishes the degree of concentration and acidity of the solution. The materials' pH falls as the number of days increases if the solution's acidity drops.

During the process of oxidative biodegradability, molecules will form CH bonds with one another. The oxidative reagent will respond with the PLA and reinforced PLA in our oxidative test, severing the materials' C-H atoms. As seen in Fig. 12a, the materials begin to break down daily as a result of the C-H bonds.

As soon as the oxidative reagent reacts with the PLA to reinforce PLA, the between molecules C-H bond breaks. The C-H bond stops to produce C+ and H-ions. When it evolves into an H-ion, it serves as a foundation. It then mixes with the CAT-ions contained in the resolution to halt the process. The redox will rise in the course of the procedure, and indoxyl will change into indigo. As shown in Fig. 12b, the pH levels of both pure PLA and reinforced PLA will rise daily due to the increase in redox.

The mass *vs*. days of PLA and PLA composite with 10%, 15% and 20% ESP are displayed in Fig. 13a. The fact that both pure PLA and reinforced composites lost mass as the number of days grew suggests that this approach is biodegradable. Comparing PLAES10 to other reinforced polymers and regular PLA, there is a noticeable bulk reduction. Hydrogen peroxide is transformed into a hydroxyl free radical through a catalytic process. The primary source of the mitochondrial oxidative respiration is the hydrogen peroxide

reactant. Hydroxyl free radicals that are produced throughout the process are extremely dangerous since they are unstable and reactive. As a catalyst, the Fe ions aid in the oxidation procedure. Organic compounds such as trichloroethylene (TCE) and tetrachloroethylene can be broken down by Fenton's reagent. As the number of days grows, pure PLA often sees a rise in pH and a drop in concentration. On the other hand, the calcium component of the reinforced PLA materials raises the pH and increases the solution's concentration. The reagent's Fe^{2+} and $CaCO_3$ mix to produce Ca^{2+} ions, increasing the solution's acidity. It is directly related to pH; as Fig. 13b shows, a daily increase in acidity will also result in a daily increase in pH.

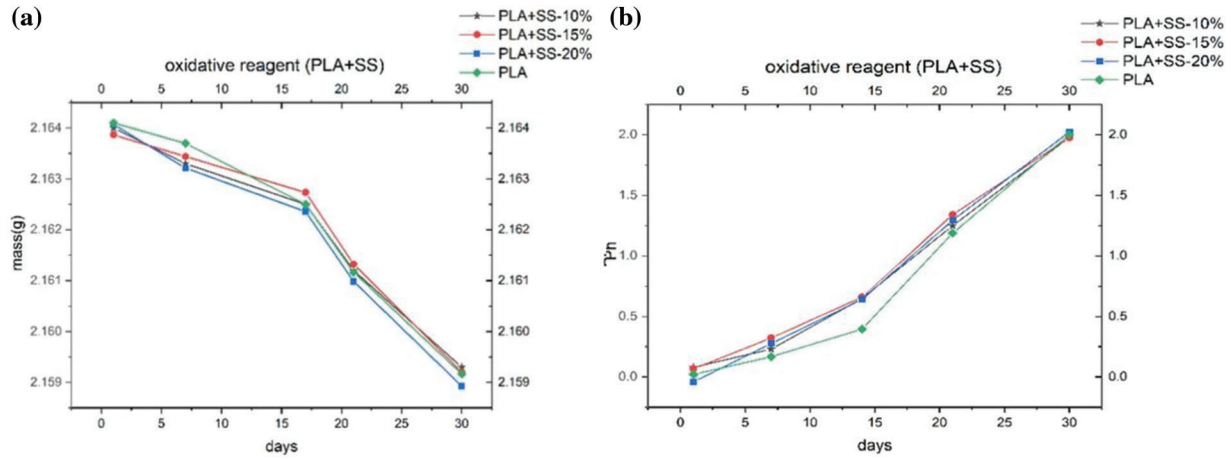

Figure 12: Test for biodegradability of oxidative reagents (a) pH *vs*. days (b) Mass *vs*. days

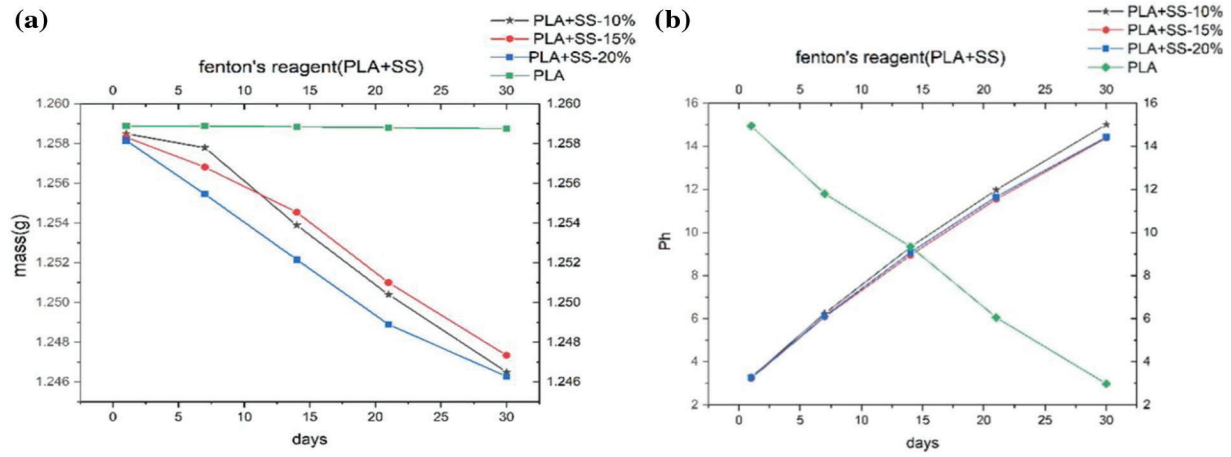

Figure 13: Test for biodegradability of Fenton's reagent (a) Mass *vs*. days (b) pH *vs*. days

4.4 X-Ray Diffraction

Fig. 14 depicts the $CaCO_3$ X-ray diffraction patterns. The overall crystalline structure and phase purity of the $CaCO_3$ particles were obtained, according to the XRD data. The XRD pattern displays the typical reflection of rhombohedral calcite. The strongest detected (hkl) peaks are at 2θ values of 23.1°, 29.4°, 36.0°, 39.4°, 43.2°, 47.5°, 48.5°, and 53.4°, which correspond to the crystallographic planes of calcite (012), (104), (110), (202), (018), (116), (122), (214), and (300), respectively. Every one of the rather sharp peaks may be classified as the usual $CaCO_3$ calcite phase. The products' exceptional purity was demonstrated by the absence of any distinctive peaks from other contaminants.

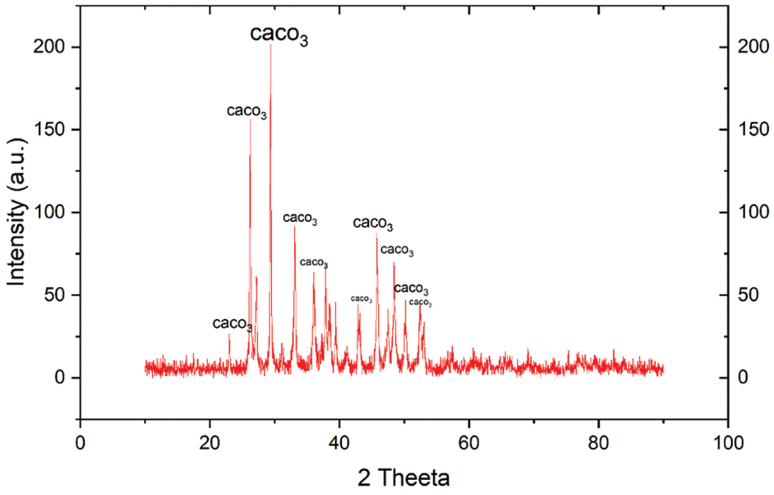

Figure 14: XRD data of sea shell powder

4.5 SEM

A detailed representation of the SEM images is given in Figs. 15–18, especially the ones that display the fractured surfaces of the pure PLA composites. The smooth, noncrinkled surface of the pure PLA SEM picture is suggestive of a brittle fracture.

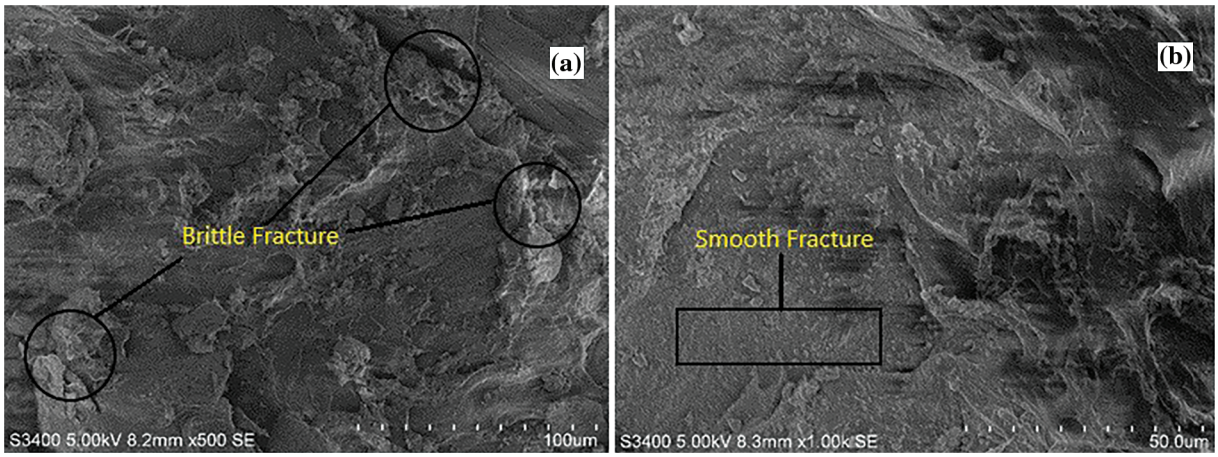

Figure 15: SEM pictures for PLA (a) Brittle fracture (b) Smooth fracture

Figs. 16–18 show the fractured surfaces of PLA + Sea Shell Powder composites, and the SEM images show a consistent dispersion and notable interaction between the two materials. The jagged morphology of sea shell powder particles, which comprises uneven form and cubical edges, is what makes them unique. A closer examination reveals that since the gaps between the filler and the polymer in both materials have closed, it indicates an effective surface interaction.

Furthermore, the SEM micrographs show particles adhering to the polymer's surface, indicating a high degree of compatibility between Sea Shell Powder and PLA. The observation of localized particle build-up suggests particle aggregation, which is likely regulated by the formation of filler interaction networks. In regions where filler loadings are larger, this tendency is particularly noticeable. To sum up, the scanning electron microscopy (SEM) examination offers significant insights into the microstructural properties of

the cracked surfaces and a thorough comprehension of the interaction between PLA and seashell powder within the composite material.

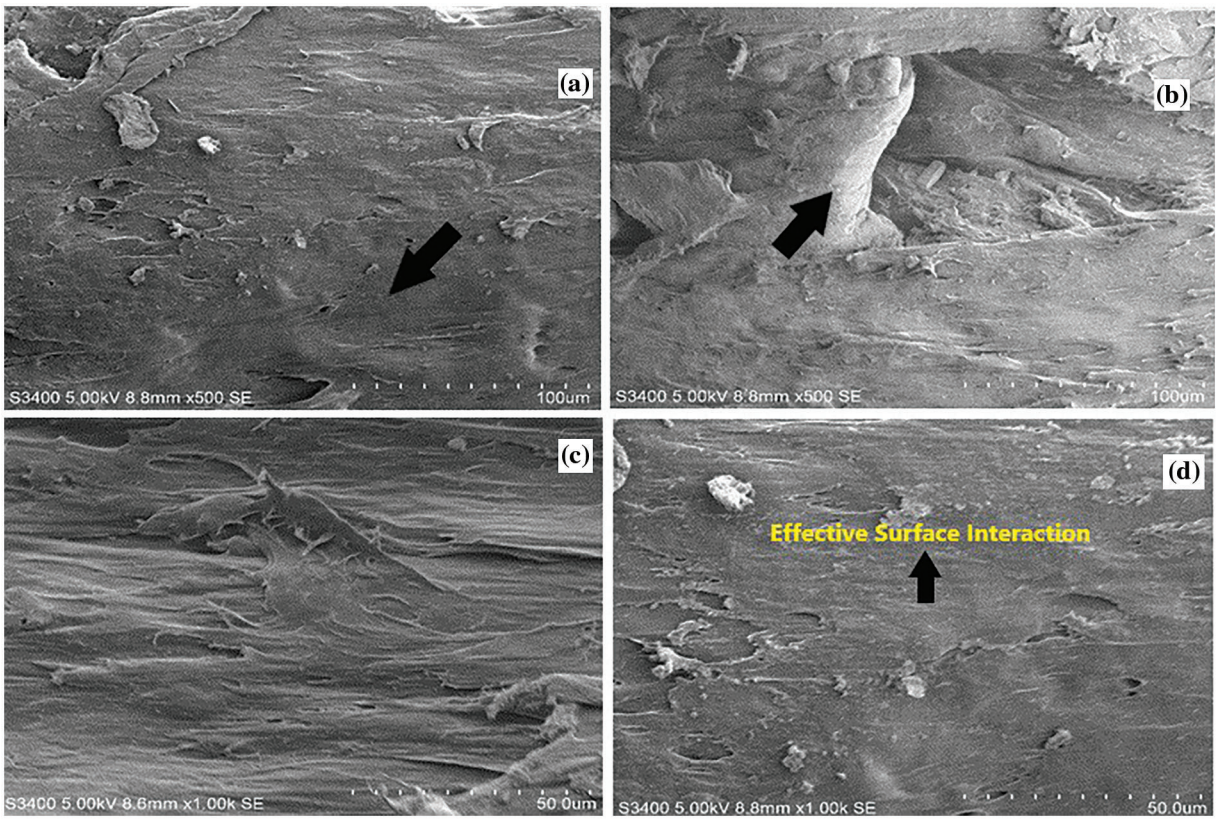

Figure 16: PLA SEM pictures using an ESP of 10% effective surface interaction at (a) and (b) magnification ×500, (c) and (d) magnification ×1000

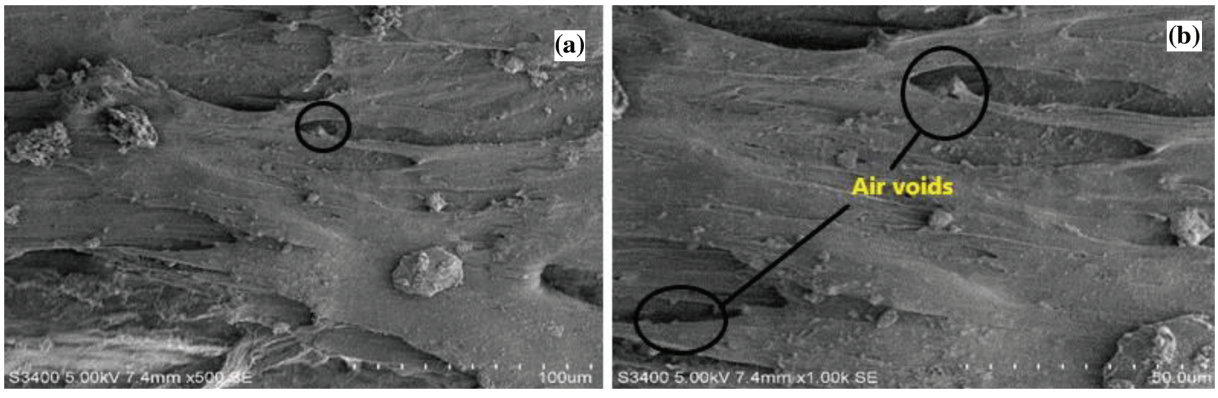

Figure 17: PLA SEM pictures with 15% ESP Air voids at (a) magnification ×500, (b) magnification ×1000

One problem encountered during the processing of Sea Shell Powder (SSP) samples was the development of a porous character in the sea shell-filled polymers, as observed in a specific region of the SEM pictures. Insufficient interfacial relations between the SSP and Polylactic Acid is indicated by voids

on the material's surface. This suggests that specific SSP pullouts and debonding in this porous structure are occurring. The composites' apparent air holes reduce their total strength. Further proof that the PLA containing SSP is dispersed equally throughout the matrix may be found in Fig. 16. The composite's reduced strength can be attributed to a variety of problems, such as insufficient dispersion of SSP, pullout phenomena, and the presence of air voids. Together, these elements also play a part in the composite's apparent porosity characteristics and reduced mechanical performance.

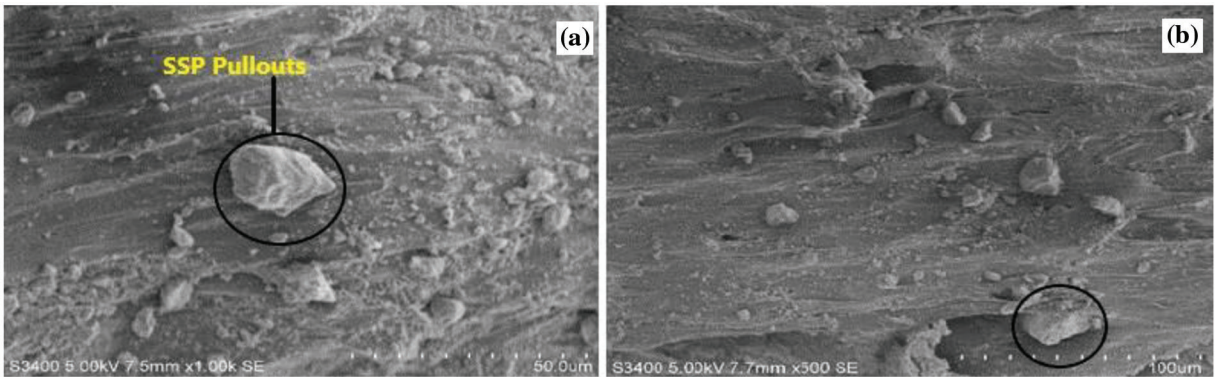

Figure 18: PLA SEM pictures with 20% ESP SSP pullouts at (a) magnification ×1000, (b) magnification ×500

5 Conclusion

The PLA-sea shell blend's tensile test findings, in summary, hold out a great deal of hope for sustainable materials. Seashells decrease PLA's tensile strength and increase modulus, but they also lessen its ductility, so it's important to properly balance these qualities in the composite formulation. The study highlights how crucial it is to distribute sea shell particles uniformly in order to guarantee reliable mechanical performance. These results provide the foundation for additional optimization, enabling the PLA-sea shell blend to be customized for particular applications that call for a particular combination of strength, flexibility, and other essential characteristics.

In particular, when it comes to addressing environmental concerns, this PLA-sea shell combination stands out as a possible substitute for traditional plastics. This material has enormous potential thanks to developments in additive manufacturing and materials science. Scholars and practitioners in the field ought to concentrate on enhancing the composition and processing of the blend in order to fully realize its potential uses, which range from enhanced biomedical gadgets to sustainable packaging. As our research indicates, achieving this goal will require more investigation and testing. The PLA-sea shell combination offers a robust and sustainable solution that combines environmental responsibility with innovation, and it may be essential in building a more resilient and environmentally responsible future.

Acknowledgement: The authors would like to thank all the colleagues and their institutions involved in this study for their valuable contributions and support. Special thanks to Crystal Feng for the publication support provided by the JRM Editorial Office.

Funding Statement: The authors received no specific funding for this study.

Author Contributions: The authors confirm their respective contributions to this paper as follows: Prashanth K P and Poornima Gubbi Shivarathri led the conceptual framework and design of the study, as well as the manuscript preparation. Prashanth K P and Rudresh M conducted the data collection and

statistical analysis. Prashanth K P, Shwetha Rajappa and Venkatesh N contributed to the literature review, experimentation and interpretation of the results. All authors reviewed the results and approved the final version of the manuscript.

Availability of Data and Materials: The datasets generated and analyzed during the current study are available from the corresponding author on reasonable request. Due to privacy concerns and ethical considerations, certain sensitive data cannot be made publicly available. However, anonymized versions of the data can be provided to researchers who meet the criteria for access to confidential information.

Ethics Approval: Not applicable.

Conflicts of Interest: The authors declare no conflicts of interest to report regarding the present study.

References

1. Ferreira PS, Ribeiro SM, Pontes R, Nunes J. Production methods and applications of bioactive polylactic acid: a review. Environ Chem Lett. 2024;22:1831–59. doi:10.1007/s10311-024-01729-z.
2. Khouri NG, Bahú JO, Blanco-Llamero C, Severino P, Concha VOC, Souto EB. Polylactic acid (PLA): properties, synthesis, and biomedical applications—A review of the literature. J Mol Struct. 2024;1309:138243. doi:10.1016/j.molstruc.2024.138243.
3. Ahmad A, Banat F, Alsafar H, Hasan SW. An overview of biodegradable poly (lactic acid) production from fermentative lactic acid for biomedical and bioplastic applications. Biomass Conv Bioref. 2024;14:3057–76. doi:10.1007/s13399-022-02581-3.
4. Li X, Lin Y, Liu M, Meng L, Li C. A review of research and application of polylactic acid composites. J Appl Polym Sci. 2023;140(7):428. doi:10.1002/app.53477.
5. Dana HR, Ebrahimi F. Synthesis, properties, and applications of polylactic acid-based polymers. Polym Eng Sci. 2023;63(1):22–43. doi:10.1002/pen.26193.
6. Joseph TM, Kallingal A, Suresh AM, Mahapatra DK, Hasanin MS, Haponiuk J, et al. 3D printing of polylactic acid: recent advances and opportunities. Int J Adv Manuf Technol. 2023;125:1015–35. doi:10.1007/s00170-022-10795-y.
7. Li G, Zhao M, Xu F, Yang B, Li X, Meng X, et al. Synthesis and biological application of polylactic acid. Molecules. 2020;25:5023. doi:10.3390/molecules25215023.
8. Jem KJ, Tan B. The development and challengesof poly (lactic acid) and poly (glycolic acid). Adv Ind Eng Polym Res. 2020;3(2):60–70. doi:10.1016/j.aiepr.2020.01.002.
9. Yao Z, Xia M, Li H, Chen T, Ye Y, Zheng H. Bivalve shell: not an abundant useless waste but a functional and versatile biomaterial. Crit Rev Environ Sci Technol. 2014;44(22):2502–30. doi:10.1080/10643389.2013.829763.
10. Saharudin SH, Shariffuddin JH, Ismail AJHM. Recovering value from waste: biomaterials production from marine shell waste. Bull Mater Sci. 2018;41:162. doi:10.1007/s12034-018-1680-5.
11. Rudresh M, Maruthi BH, Channakeshavalu K, Nagaswarupa HP. Mechanical and thermal behavior of epoxy based halloysite nano clay/PMMA hybrid nanocomposites. SN Appl Sci. 2019;1:687. doi:10.1007/s42452-019-0749-0.
12. Ramnath BV, Jeykrishnan J, Ramakrishnan G, Barath B, Ejoelavendhan E, Raghav PA. Sea shells and natural fibres composites: a review. Mater Today: Proc. 2018;5(1):1846–51. doi:10.1016/j.matpr.2017.11.284.
13. Yang X-M, Qiu S, Yusuf A, Sun J, Zhai Z, Zhao J, et al. Recent advances in flame retardant and mechanical properties of polylactic acid: a review. Int J Biol Macromol. 2023;243:125050. doi:10.1016/j.ijbiomac.2023.125050.
14. Rubežić MZ, Krstić AB, Stanković HZ, Ljupković RB, Ranđelovic MS, Zarubica AR. Different types of biomaterials: structure and application: a short review. Adv Technol. 2020;9(1):69–79. doi:10.5937/savteh2001069R.

15. Habte L, Khan MD, Shiferaw N, Farooq A, Lee M-H, Jung S-H, et al. Synthesis, characterization and mechanism study of green aragonite crystals from waste biomaterials as calcium supplement. Sustainability. 2020;12(12):5062. doi:10.3390/su12125062.
16. Hembrick-Holloman V, Samuel T, Mohammed Z, Jeelani S, Rangari VK. Ecofriendly production of bioactive tissue engineering scaffolds derived from egg- and sea-shells. J Mater Res Technol. 2020;9(6):13729–39. doi:10.1016/j.jmrt.2020.09.093.
17. Vecchio KS, Zhang X, Massie JB, Wang M, Kim CW. Conversion of bulk seashells to biocompatible hydroxyapatite for bone implants. Acta Biomater. 2007;3(6):910–8. doi:10.1016/j.actbio.2007.06.003.
18. Lee S-W, Balázsi C, Balázsi K, Seo D-H, Kim HS, Kim C-H, et al. Comparative study of hydroxyapatite prepared from seashells and eggshells as a bone graft material. Tissue Eng Regen Med. 2014;11:113–20. doi:10.1007/s13770-014-0056-1.
19. Hanumantharaju HG, Prashanth KP, Ramu B, Venkatesh N, Chethan GR. 3D printing of biopolymer composites investigation on effect of egg shell particles on polylactic acid matrix. Biointerface Res Appl Chem. 2022;13:1–16. doi:10.33263/BRIAC133.251.
20. Razali MS, Khimeche K, Melouki R, Boudjellal A, Vroman I, Alix S, et al. Preparation and properties enhancement of poly (lactic acid)/calcined-seashell biocomposites for 3D printing applications. J Appl Polym Sci. 2022;139(5):51591. doi:10.1002/app.51591.
21. Castanon-Jano L, Palomera-Obregon P, Lazaro M, Blanco-Fernandez E, Blason S. Enhancing sustainability in polymer 3D printing via fusion filament fabrication through integration of by-products in powder form: mechanical and thermal characterization. Int J Adv Manuf Technol. 2024;133:1251–69. doi:10.1007/s00170-024-13635-3.
22. Abdallah YK, Estévez AT. Biowelding 3D-printed biodigital brick of seashell-based biocomposite by pleurotus ostreatus mycelium. Biomimetics. 2023;8(6):504. doi:10.3390/biomimetics8060504.
23. Padole M, Gharde S, Kandasubramanian B. Three-dimensional printing of molluscan shell inspired architectures via fused deposition modeling. Environ Sci Pollut Res. 2021;28:46356–66. doi:10.1007/s11356-020-09799-6.
24. Hussain PS, Shah ZA, Sabiruddin K, Keshri AK. Characterization and tribological behaviour of Indian clam seashell-derived hydroxyapatite coating applied on titanium alloy by plasma spray technique. J Mech Behav Biomed Mater. 2023;137:105550. doi:10.1016/j.jmbbm.2022.105550.
25. Nurazzi NM, Norrrahim MNF, Mulla MH, Kamarudin SH, Rani MSA, Rushdan AI, et al. Mechanical performance of seashell-reinforced polymer composites for structural applications. In: Polymer composites derived from animal sources. Woodhead Publishing; 2024. p. 243–57. doi:10.1016/B978-0-443-22414-0.00013-2.
26. Nirmal N, Demir D, Ceylan S, Ahmad S, Goksen G, Koirala P, et al. Polysaccharides from shell waste of shellfish and their applications in the cosmeceutical industry: a review. Int J Biol Macromol. 2024;265:131119. doi:10.1016/j.ijbiomac.2024.131119.
27. Singh AAMM, Franco PA, Azhagesan N, Sharun V. Exploring seashell and rice husk waste for lightweight hybrid biocomposites: synthesis, microstructure, and mechanical performance. Biomass Conv Bioref. 2023;21:81. doi:10.1007/s13399-023-04846-x.
28. Homavand A, Cree DE, Wilson LD. Polylactic acid composites reinforced with Eggshell/$CaCO_3$ filler particles: a review. Waste. 2024;2(2):169–85. doi:10.3390/waste2020010.
29. Cree D, Owuamanam S, Soleimani M. Mechanical properties of a bio-composite produced from two biomaterials: polylactic acid and brown eggshell waste fillers. Waste. 2023;1(3):740–60. doi:10.3390/waste1030044.
30. Yathrib A, AL-Salman HNK, Ali MH, Mohammed KJ, Sherzod A, Alaa AO, et al. Effect and investigating of graphene nanoparticles on mechanical, physical properties of polylactic acid polymer. Case Studies Chem Environ Eng. 2024;9:100612. doi:10.1016/j.cscee.2024.100612.
31. Sun Y, Yu B, Liu Y, Cheng B, Wang J, Yan J, et al. Novel bio-based nanosheets: improving the fire safety, electromagnetic shielding and mechanical properties of polylactic acid. Compos Part A: Appl Sci Manuf. 2024;179:108044. doi:10.1016/j.compositesa.2024.108044.
32. Begum SA, Krishnan PSG, Kanny K. Properties of poly (lactic Acid)/ hydroxyapatite biocomposites for 3D printing feedstock material. J Thermoplastic Compos Mater. 2024;37(2):644–68. doi:10.1177/08927057231182165.

33. Zhao T, Yu J, Zhang X, Han W, Zhang S, Pan H, et al. Thermal, crystallization, and mechanical properties of polylactic acid (PLA)/poly(butylene succinate) (PBS) blends. Polym Bull. 2024;81:2481–504. doi:10.1007/s00289-023-04848-9.
34. Mocanu A-C, Constantinescu A-E, Pandele M-A, Voicu ŞI, Ciocoiu R-C, Batalu D, et al. Biocompatible composite filaments printable by fused deposition modelling technique: selection of tuning parameters by influence of biogenic hydroxyapatite and graphene nanoplatelets ratios. Biomimetics. 2024;9(3):189. doi:10.3390/biomimetics9030189.
35. Narain Kumar S, Kaaviya J, Sabarinathan P, Mostafizur R, Saravanan P. Tribological performance of the novel 3D printed PLA/Almond shell particles added PLA Single Gradient Functionally Graded Material (SGFGM). Mater Today Commun. 2024;40:109611. doi:10.1016/j.mtcomm.2024.109611.
36. Palaniyappan S, Sivakumar NK, Sekar V. Sustainable approach to the revalorization of crab shell waste in polymeric filament extrusion for 3D printing applications. Biomass Conv Bioref. 2023;14:15721–38. doi:10.1007/s13399-023-03795-9.
37. Liu Z, Lei Q, Xing S. Mechanical characteristics of wood, ceramic, metal and carbon fiber-based PLA composites fabricated by FDM. J Mater Res Technol. 2019;8:3741–51. doi:10.1016/j.jmrt.2019.06.034.
38. Alok Kumar T, Gupta MK, Harinder S. PLA based biocomposites for sustainable products: a review. Adv Ind Eng Polym Res. 2023;6(4):382–95. doi:10.1016/j.aiepr.2023.02.002.
39. Singh R, Kumar R, Farina I, Colangelo F, Feo L, Fraternali F. Multi-material additive manufacturing of sustainable innovative materials and structures. Polymers. 2019;11:62. doi:10.3390/polym11010062.
40. Kumar KSS, Vivekananthan M, Saravanakumar M, Raj FS. Investigation of physico chemical, mechanical and thermal properties of the guettarda speciosa bark fibers. Mater Today: Proc. 2021;37:1845–9. doi:10.1016/j.matpr.2020.07.443.
41. Ashok B, Naresh S, Reddy KO, Madhukar K, Cai J, Zhang L, et al. Tensile and thermal properties of poly (lactic acid)/Eggshell powder composite films. Int J Polym Anal Charact. 2014;19:245–55. doi:10.1080/1023666X.2014.879633.
42. Backes EH, Pires LDN, Costa LC, Passador FR, Pessan LA. Analysis of the degradation during melt processing of PLA/biosilicate composites. J Compos Sci. 2019;3:52. doi:10.3390/jcs3020052.
43. Prashanth KP, Hanumantharaju HG, Bakshi R. Bio-materials science and engineering: basic theory with engineering applications. Saarbrucken, Germany: LAMBERT Academic Publishing; 2020.
44. Segun A, Adewuyi B, Ojo D, Gideon O. Mechanical and structural properties of nanocarbon particles reinforced in plasticised polylactic acid for high strength application. J Phys Sci. 2021;32:41–56. doi:10.21315/jps2021.32.2.4.
45. Omran A, Mohammed A, Sapuan S, Ilyas R, Asyraf M, Rahimian Koloor S, et al. Micro-and nanocellulose in polymer composite/materials: a review. Polymers. 2021;13:231. doi:10.3390/polym13020231.
46. Prashanth KP, Rudresh M, Surendra BS, Rashmi A. Ceramic coating materials: introduction, materials and characterization techniques. In: Advanced ceramic coatings for energy applications. Elsevier; 2024. vol. 51, p. 1–15. doi:10.1016/B978-0-323-99620-4.00001-4.
47. Khalid S, Yu L, Meng L, Liu H, Ali A, Chen L. Poly (lactic acid)/starch composites: effect of microstructure and morphology of starch granules on performance. J Appl Polym Sci. 2017;134(46). doi:10.1002/app.45504.
48. Khalid S, Yu L, Feng M, Meng L, Bai Y, Ali A, et al. Development and characterization of biodegradable antimicrobial packaging films based on polycaprolactone, starch and pomegranate rind hybrids. Food Packag Shelf Life. 2018;18:71–9. doi:10.1016/j.fpsl.2018.08.008.
49. Hemanth B, Hanumantharaju HG, Prashanth KP, Sanman S, Lavakumar KS. FEA analysis of TI-6AL-4V and 30% collagen reinforced PMC used as biomaterials for ankle implants. Biointerface Res Appl Chem. 2022;13(4):378. doi:10.33263/BRIAC134.378.